Linear-to-Circular Polarization Converter Based on Four-Arms Star FSS at 5.2 GHz for 5G Applications

Deisy Formiga Mamedes[1], Jens Bornemann[1], Alfredo Gomes Neto[2]
[1] Department of Electrical and Computer Engineering, University of Victoria, Victoria, Canada, mamedes@uvic.ca, j.bornemann@ieee.org
[2] Department of Electrical Engineering, Federal Institute of Paraiba, João Pessoa, Brazil, alfredogomes@ifpb.edu.br

***Abstract*—A single-layer frequency selective surface (FSS) polarizer is proposed as a linear-to-circular polarization converter, operating at 5.2 GHz for 5G applications. The analyses are based on the magnitude and phase of the transmission coefficient of two orthogonal electric field components. The four-arms star geometry used in the FSS polarizer is simple to design, and equations are provided. The design approach is validated by a good agreement between numerical and measured results.**

***Index Terms*—polarization converter, linear polarization, polarizer, circular polarization, cross-polarization, frequency selective surfaces.**

I. Introduction

In communication systems, the use of circular polarization (CP) circuitries has demonstrated to be a viable solution to overcome some disruptions such as susceptibility to multi-path fading, atmospheric absorptions, and polarization mismatch [1], [2]. The conversion of linear polarization (LP) to CP has attracted the interest of engineers, and its principle consists of the use of two orthogonal linearly polarized field components with equal amplitude and a 90° phase difference. To achieve the conversion to CP, different polarizer structures have been reported such as Fabry-Perot cavities [3], meander-line [4], [5] and SIW circuits [6], etc.

Frequency selective surface (FSS) polarizers offer low-profile and easy fabrication, making them favorable among periodic structures. FSSs are composed of metal elements etched on a dielectric substrate, arranged in a planar periodic structure. The FSS frequency response depends on the substrate thickness h, relative permittivity ε_r, the geometry of the unit cell element, the spacing between the elements within the structure, and the polarization of the incident wave [7], Fig. 1.

The geometries among the types of FSS polarizers are mainly based on cross-dipole [8] or ring shapes [9], and also on cascade structures [10], [11]. In this paper, a linear-to-circular polarization (LP-to-CP) converter based on a single-layer FSS is proposed. The elements of the FSS are based on the four-arms star geometry that can be easily designed.

II. FSS Polarizer Design

The condition for the outgoing wave to be circularly polarized is that an incident electric field, E_i, oriented at 45° with two decomposed vector components, i.e., E_{ix} (horizontal) and E_{iy} (vertical), experience a 90° phase difference ($\Phi_y - \Phi_x = 90°$) while propagating through the polarizer, as shown in Fig. 2.

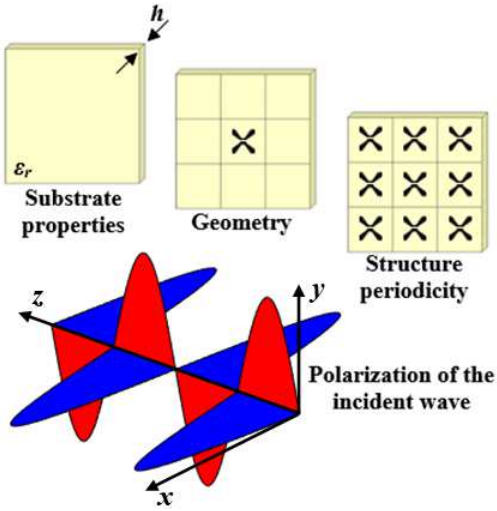

Fig. 1. Parameters that affect the FSS frequency response.

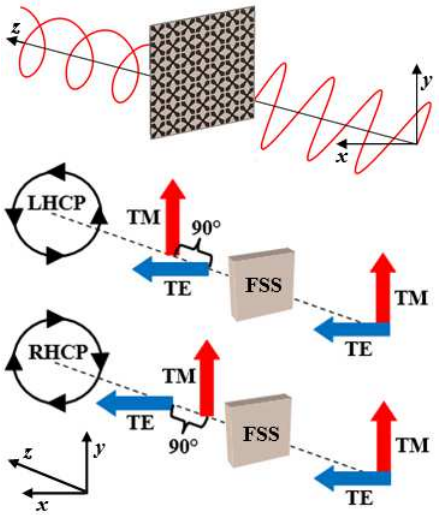

Fig. 2. Operation principle of the linear-to-circular polarizer.

To categorize the outgoing wave at the output of the polarizer as left-handed circular polarization (LHCP) or right-handed circular polarization (RHCP), the superposition

of the transverse electric (TE) and transverse magnetic (TM) components is analyzed. If the transmission of the TM component occurs with 90° phase ahead of the TE component, the wave will be LHCP. The opposite happens when the TE component is transmitted 90° in advance of the TM component, then the wave will be RHCP.

The FSS polarizer proposed in this paper is based on the four-arms star geometry, which has previously shown its ability to reconfigure antenna radiation patterns [12], [13] and FSSs [14], [15], as well as to enhance antenna gain [16]. The geometry of the unit cell of this FSS and its parameters are illustrated in Fig. 3. Initially, the unit cell dimension is defined as $W_x = W_y$, approximately a third of a wavelength, and then a rectangular patch is designed as $L_x = L_y$, where the arms are shaped. From the edges, lines cross the rectangular patch with $d_x = d_y$, and the four-arms star geometry is achieved. A square patch of $s_x = s_y$ is positioned in the center of the unit cell, with a gap of g to provide an asymmetric geometry when comparing x- and y-directions.

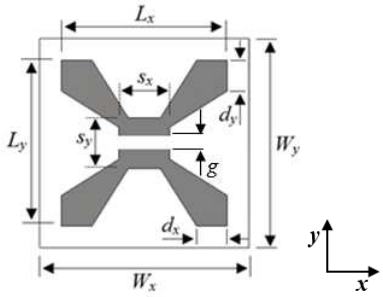

Fig. 3. Geometry and parameters of the four-arms star FSS unit cell.

The design process to determine the first resonant frequencies for the TE and TM modes of the four-arms star FSS can be carried out using the following steps:

1. The size of the arms defines the resonant frequency for the TM polarization according to

$$f_{TM}(GHz) = \frac{0.3}{(Lx + Ly)\sqrt{\varepsilon_{r_{eff}}}} \tag{1}$$

Ref. [17] presents an interpolating formula that fits the variation of the effective permittivity

$$\varepsilon_{r_{eff}} = \varepsilon_r + (\varepsilon_r - 1)\left[\frac{-1}{e^{\frac{10h}{W}N}}\right] \tag{2}$$

which considers the dielectric permittivity and thickness of the substrate, periodicity W ($W = W_x = W_y$), and the exponential factor, N, of the unit cell filling. For the geometry proposed, the value of N is 1.9.

2. For the TE polarization, the E-field is maximum in the center of the unit cell, and the gap is seen now as an additional capacitance to the circuit, making its resonant frequency appear as

$$f_{TE}(GHz) = 1.8 f_{TM} \tag{3}$$

Note that the factor of 1.8 in Eq. (3) is an approximation based on the gap of 1 mm used in this design. Other gap widths will lead to different factors.

III. Results

The numerical characterizations were obtained through the commercial software package ANSYS. The FSS was designed on a low-cost FR-4 fiber-glass dielectric substrate with $\varepsilon_r = 4.4$, $h = 0.762$ mm, and the dimensions of the structure are $W_x = W_y = 30$ mm, $L_x = L_y = 26$ mm, $d_x = d_y = s_x = s_y = 6$ mm, and $g = 1$ mm. The FSS was manufactured to validate the numerical results by experiments. The prototype was fabricated with 7 × 7 elements and overall dimensions of 21 cm × 21 cm, as shown in Fig. 4 with an additional enlargement of the unit cell.

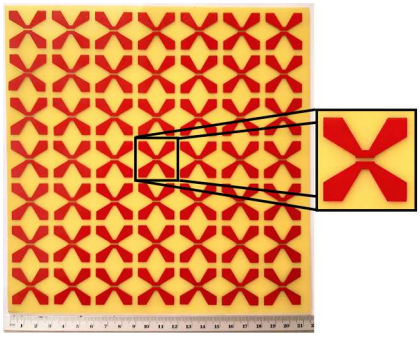

Fig. 4. Fabricated FSS and individual cell.

Measurements were carried out in the GTEMA/IFPB microwave measurements laboratory (Fig. 5a), using an Agilent E5071C Vector Network Analyzer, two SAS-571 double ridge horn antennas, spaced with 160 cm apart, and a measurement window with pyramidal radiation-absorbent material surrounding it. A normal wave incidence to the FSS is considered in Fig. 5a. Fig. 5b shows the measurement setup to measure cross-polarization with the FSS rotated by 45°.

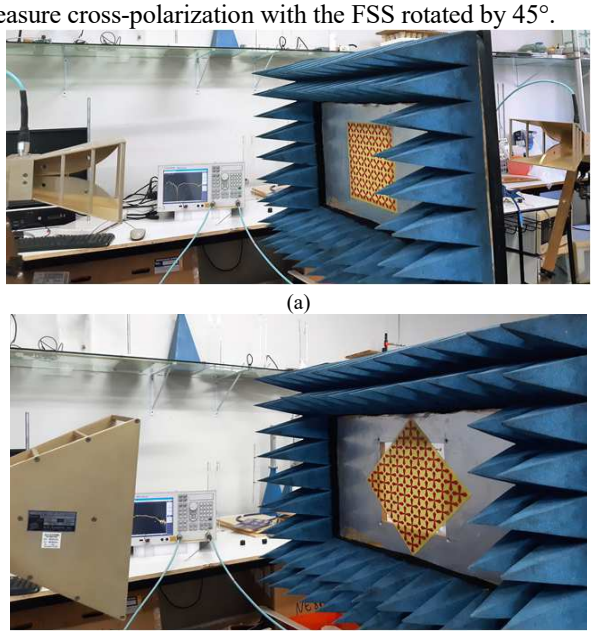

(a) (b)

Fig. 5. Measurement setup for FSS tilted by (a) $\phi = 0°$ and (b) $\phi = 45°$.

The four-arms star geometry with a gap is polarization dependent, and results for the transmission coefficients are presented in this section. From (1), the proposed FSS was designed for 3.8 GHz for the TM polarization and, with the additional gap in the center, the resonant frequency for the TE polarization is 6.84 GHz, according with (3). Fig. 6 shows the simulated transmission coefficient along with the measured results. The measured resonant frequencies are f_{TM} = 3.83 GHz and f_{TE} = 6.97 GHz, demonstrating a good agreement with those obtained numerically (f_{TM} = 3.82 GHz and f_{TE} = 7.14 GHz), with a maximum difference of 0.26 % and 2.38 %, respectively. To achieve circular polarization, one of the conditions is that the magnitude of TE and TM modes must be identical at the operating frequency. Note that the magnitudes of TE and TM modes are nearly equal at 5.2 GHz with -3-dB transmission.

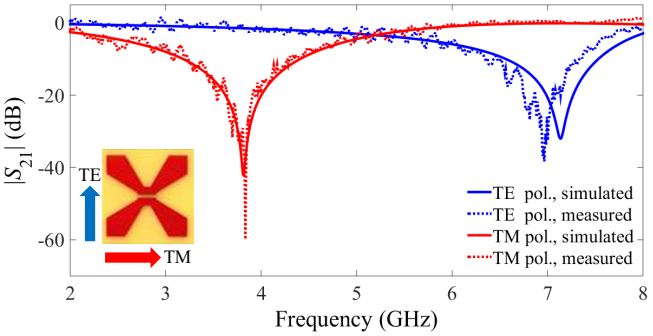

Fig. 6. Simulated and measured results for the magnitude of the transmission coefficient of the orthogonal components of the E-field.

The gap separating the top part of the FSS from its bottom part produces a capacitive effect, which makes the TM mode lead the TE mode with a phase difference between them. The other condition for circular polarization to occur is that after the incoming wave passes through the polarizer, the phase difference between the two E-field component must be 90° (or odd multiples thereof). Fig. 7 presents the simulated and measured phase transmission coefficients of the two orthogonal field components for the proposed FSS. The results show a phase difference of nearly of 90° between the TE and TM modes, indicating that circular polarization appears at 5.2 GHz.

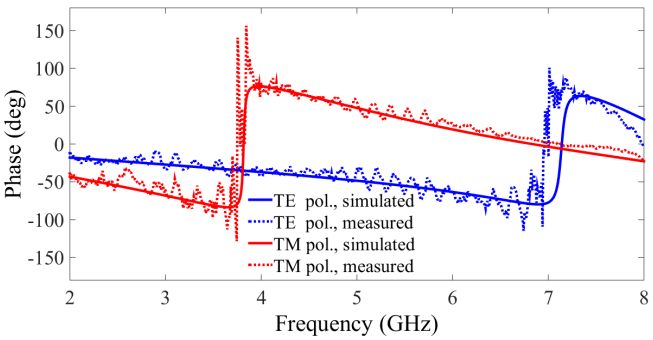

Fig. 7. Simulated and measured results for the phases of the transmission coefficients of the orthogonal components of the E-field.

The proposed FSS polarizer efficiency was confirmed through simulated and measured results. For this case, the FSS is rotated by 45° as shown in Fig. 5b. The co- (vertical) and cross-polarization (horizontal) responses of the FSS are illustrated in Fig. 8. An attenuation of 6 dB is observed at 5.2 GHz which includes the 3-dB verified in Fig. 6. Note that the power of the incoming vertical polarization divides along the TE (+45°) and TM (-45°) polarizations. That is confirmed by nearly the same co- and cross-polarization measurements of 6-dB attenuation. The results obtained experimentally follow the curves of the numerical ones in reasonable agreement.

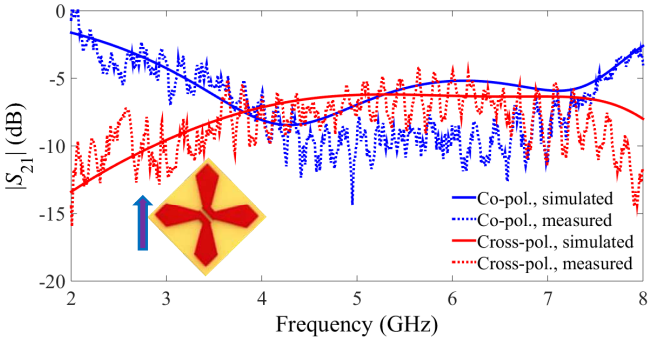

Fig. 8. Simulated and measured results of the co- (vertical) and cross-polarized (horizontal) components.

The simulated and measured results of the 3-dB axial ratio (AR) bandwidth are presented in Fig. 9 where the AR was obtained using the well-known equations presented in [18]. The minimum AR occurs at 5.22 GHz (0.19 dB) and 5.21 GHz (0.02 dB) for the numerical and measured results, respectively. The bandwidth for AR < 3 dB is 1.6 GHz (experimentally) and 1.56 GHz (numerically).

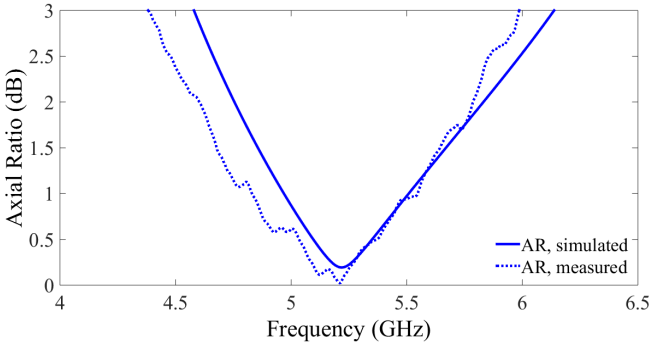

Fig. 9. Simulated and measured axial ratio of the proposed polarizer.

Table I compares the proposed FSS converter with previous works available in the literature in terms of number of metal layers, reconfigurability and electrical size. The proposed FSS polarizer demonstrates a good performance; when compared to other converters, it proposes a geometry that can be easily designed, and it just uses a single metalized substrate. Both RHCP or LHCP can be achieved by rotating the direction of the FSS by 90°.

TABLE I. COMPARISON BETWEEN THE DESIGNED POLARIZATION CONVERTER AND PREVIOUS WORKS

Ref.	Frequency (GHz)	Number of layers	Reconfigurable	Dimension of unit cell
[19]	10	5	Yes	$0.33\lambda_0$
[20]	9	4	No	$0.45\lambda_0$
[21]	10	2	No	$0.24\lambda_0$
This work	5.2	1	No	$0.52\lambda_0$

IV. CONCLUSION

In this paper a linear-to-circular polarization converter is proposed, operating at 5.2 GHz for 5G applications. It is demonstrated that a single-layer FSS based on the four-arms star geometry can be used as the polarizing element. The design process of the FSS polarizer includes simulations in ANSYS tools and experimental verifications. The gap splitting the four-arms geometry in two pairs introduces a capacitive effect to the circuit. The added capacitance provides a phase difference of 90° between the TE and TM modes. The results show that the TE mode lags the TM mode, which makes the outgoing wave from the polarizer to be LHCP. The design approach, including expressions for a first and fast design of the four-arms star geometry, is described and validated with numerical and experimental results.

REFERENCES

[1] Y. Wang and A. Zhang, "Dual circularly polarized Fabry–Perot resonator antenna employing a polarization conversion metasurface," *IEEE Access*, vol. 9, pp. 44881-44887, 2021, doi: 10.1109/ACCESS.2021.3062460.

[2] P. Xie, G. Wang, H. Li, X. Gao, and B. Zong, "A novel method for circularly polarized Fabry-Perot cavity antenna," *Proc. Int. Conf. Microw. Millim. Wave Techn.* (ICMMT), Shanghai, China, Sep. 2020, pp. 1-3, doi: 10.1109/ICMMT49418.2020.9386767.

[3] Z. Liu, Z. Cao, and L. Wu, "Compact low-profile circularly polarized Fabry–Perot resonator antenna fed by linearly polarized microstrip patch," *IEEE Antennas Wirel. Propagat. Lett*., vol. 15, pp. 524-527, 2016, doi: 10.1109/LAWP.2015.2456886.

[4] L. Young, L. Robinson, and C. Hacking, "Meander-line polarizer," *IEEE Trans. Antennas Propagat*., vol. 21, no. 3, pp. 376-378, May 1973, doi: 10.1109/TAP.1973.1140503.

[5] P. Fei, Z. Shen, X. Wen, and F. Nian, "A single-layer circular polarizer based on hybrid meander line and loop configuration," *IEEE Trans. Antennas Propagat*., vol. 63, no. 10, pp. 4609-4614, Oct. 2015, doi: 10.1109/TAP.2015.2462128.

[6] E. Arnieri, F. Greco, L. Boccia, and G. Amendola, "A SIW-based polarization rotator with an application to linear-to-circular dual-band polarizers at K-/Ka-band," *IEEE Trans. Antennas Propagat*., vol. 68, no. 5, pp. 3730-3738, May 2020, doi: 10.1109/TAP.2020.2963901.

[7] B. A. Munk, *Frequency Selective Surfaces: Theory and Design*. New York: Wiley, 2000.

[8] G. I. Kiani and V. Dyadyuk, "Quarter-wave plate polariser based on frequency selective surface," *Proc. 40th European Microwave Conference*, Paris, France, Sep. 2010, pp. 1361-1364, doi: 10.23919/EUMC.2010.5616657.

[9] M. Euler, V. Fusco, R. Cahill, and R. Dickie, "325 GHz single layer sub-millimeter wave FSS based split slot ring linear to circular polarization converter," *IEEE Trans. Antennas Propagat*., vol. 58, no. 7, pp. 2457-2459, July 2010, doi: 10.1109/TAP.2010.2048874.

[10] M. Euler, V. Fusco, R. Cahill, and R. Dickie, "FSS based sub-millimetre wave spatial phase shifter design considerations," Proc. 3rd Eur. Conf. Antennas Propagat., Berlin, Germany, Mar. 2009, pp. 1648-1650.

[11] J. Bornemann, "Computer-aided design of multilayered dielectric frequency-selective surfaces for circularly polarized millimeter-wave applications," *IEEE Trans. Antennas Propagat*., vol. 41, no. 11, pp. 1588-1591, Nov. 1993, doi: 10.1109/8.267362.

[12] D. F. Mamedes, A. G. Neto, and J. Bornemann, "Reconfigurable corner reflector using PIN-diode-switched frequency selective surfaces," *IEEE AP-S Int. Sym. Dig.*, Montreal, Canada, July 2020, pp. 127-128, doi: 10.1109/IEEECONF35879.2020.9329791.

[13] D. F. Mamedes and J. Bornemann, "High-gain reconfigurable antenna system using PIN-diode-switched frequency selective surfaces for 3.5 GHz 5G application," *Proc. SBMO/IEEE MTT-S Int. Microw. Optoelectron. Conf.* (IMOC), Fortaleza, Brazil, Oct. 2021, in press.

[14] D. F. Mamedes, A. G. Neto, J. C. e Silva, and J. Bornemann, "Design of reconfigurable frequency-selective surfaces including the PIN diode threshold region," *IET Microw., Antennas Propag.*, vol. 12, no. 9, pp. 1483-1486, 2018, doi.org/10.1049/iet-map.2017.0761.

[15] A. G. Neto, J. C. e Silva, A. G. Barboza, D. F. Mamedes, I. B. G. Coutinho, and M. de Oliveira Alencar, "Varactor-tunable four arms star bandstop FSS with a very simple bias circuit," *Proc. 13th Eur. Conf. Antennas Propagat.* (EuCAP), Krakow, Poland, Mar./Apr. 2019, pp. 1-5.

[16] D. F. Mamedes and J. Bornemann, "Gain enhancement of bio-inspired antenna using FSS for 28 GHz 5G application," *Proc. SBMO/IEEE MTT-S Int. Microw. Optoelectron. Conf.* (IMOC), Fortaleza, Brazil, Oct. 2021, in press.

[17] F. Costa, A. Monorchio, and G. Manara, "Efficient analysis of frequency-selective surfaces by a simple equivalent-circuit model," *IEEE Antennas Propagat. Mag.*, vol. 54, no. 4, pp. 35-48, Aug. 2012, doi: 10.1109/MAP.2012.6309153.

[18] T. Kitsuregawa, *Advanced technology in satellite communication antennas: electrical and mechanical design*. Artech House, Norwood, USA, 1990.

[19] L. Li, Y. Li, Z. Wu, F. Huo, Y. Zhang and C. Zhao, "Novel polarization-reconfigurable converter based on multilayer frequency-selective surfaces," *Proc. IEEE*, vol. 103, no. 7, pp. 1057-1070, July 2015, doi: 10.1109/JPROC.2015.2437611.

[20] W. Zhang, J. -Y. Li, and J. Xie, "A broadband circular polarizer based on cross-shaped composite frequency selective surfaces," *IEEE Trans. Antennas Propagat.*, vol. 65, no. 10, pp. 5623-5627, Oct. 2017, doi: 10.1109/TAP.2017.2735459.

[21] W. Li, Y. Lan, H. Wang, and Y. Xu, "Microwave polarizer based on complementary split ring resonators frequency-selective surface for conformal application," *IEEE Access*, vol. 9, pp. 111383-111389, 2021, doi: 10.1109/ACCESS.2021.3102942.